Optics & Laser Technology 143 (2021) 107301

Contents lists available at ScienceDirect

Optics and Laser Technology

journal homepage: www.elsevier.com/locate/optlastec

Full length article

Single quantum emitters detection with amateur CCD: Comparison to a scientific-grade camera

Anton S. Gritchenko [a,b], Ivan Yu. Eremchev [a,c], Andrey V. Naumov [a,c,d,*], Pavel N. Melentiev [a,b], Victor I. Balykin [a,b]

[a] Institute of Spectroscopy Russian Academy of Sciences, 108840 Fizicheskaya str., 5, Troitsk, Moscow, Russia
[b] National Research University, Higher School of Economics, 101000, Myasnitskaya str., 20, Moscow, Russia
[c] Moscow State Pedagogical University, 119435, Malaya Pirogovskaya 1/1, Moscow, Russia
[d] P.N. Lebedev Physical Institute of the Russian Academy of Sciences, Troitsk Branch, 108840, Fizicheskaya Str., 11, Troitsk, Moscow, Russia

ARTICLE INFO

Keywords:
Photonics
Microscopy
Fluorescence nanoscopy
Imaging
CCD
CMOS
Sensor
Detector
SNR
SPS
Single molecule
Quantum dots
Color centers
NV
SiV
GeV
Price-to-quality

ABSTRACT

Fluorescence imaging of single quantum light emitters (atoms, molecules, quantum dots, color centers in crystals) is an inherent experimental problem of modern photonics and its numerous applications. In these measurements, highly sensitive cameras are of the key significance. Recent progress in technologies of charge-coupling devices (CCD) and complementary metal-oxide semiconductor (CMOS) sensors opens up possibilities for detection of extreme low light signals up to a single photon counting. Here, we investigate the parameters of high-professional scientific- and amateur-grade cameras in the view of their use in the fluorescence nanoscopy with the detection of single molecules and, in general, quantum emitters of different nature. A series of photoluminescence imaging experiments have been conducted with single colloidal semiconductor core-shell nanocrystals CdSeS/ZnS (quantum dots, QD), which are usually considered as a basis of various sensors and actuators technologies. We find parameters of the experiment for the amateur-grade camera to obtain images of single QDs with signal-to-noise ratio compared to the scientific-grade camera at exposure times ranging from 1s to 1000s.

1. Introduction

Detection, visualization and measurement of spectral properties of single quantum emitters is increasingly developing and becoming a key element for methods and devices of modern photonics and numerous interdisciplinary applications. Thus, the ability to detect the radiation of individual atoms, molecules, nanoparticles is of high demand in quantum technologies (single photon sources) [1], medical and bio diagnostics (fluorescent nanoscopy) [2,3], nanosensorics [4], solid state physics [5,6,7,8], chemistry [9], micro- and nanostructure physics [10,11,12,13,14], nanophotonics [15], nanoplasmonics [16], as well as various combined microscopy techniques [17].

The possibility of single quantum emitters detection is determined by two main parameters: (1) the emitters photon flux, which is typically in the range of 10^5–10^7 photons/s [18,19,20], and (2) optical setup efficiency (5–40%), which is determined by the numerical aperture of a microscope objective, the internal system loss (on dielectric filters used to distinguish low intensity quantum emitters fluorescence from high intensity exciting laser radiation) and the quantum efficiency of a detector [21].

A CCD camera is one of the key elements affecting optical setup efficiency. The variety of cameras offered today is schematically represented on Fig. 1. All cameras can be conventionally divided into three categories: (1) mass market cameras, a prominent representative of which are cameras in modern mobile phones, mobile devices and laptops, CCTV surveillance, etc., the main advantage of which is their low

* Corresponding author.
E-mail address: a_v_naumov@mail.ru (A.V. Naumov).
URL: https://www.single-molecule.ru (A.V. Naumov).

https://doi.org/10.1016/j.optlastec.2021.107301
Received 26 January 2021; Received in revised form 16 May 2021; Accepted 30 May 2021
Available online 17 June 2021

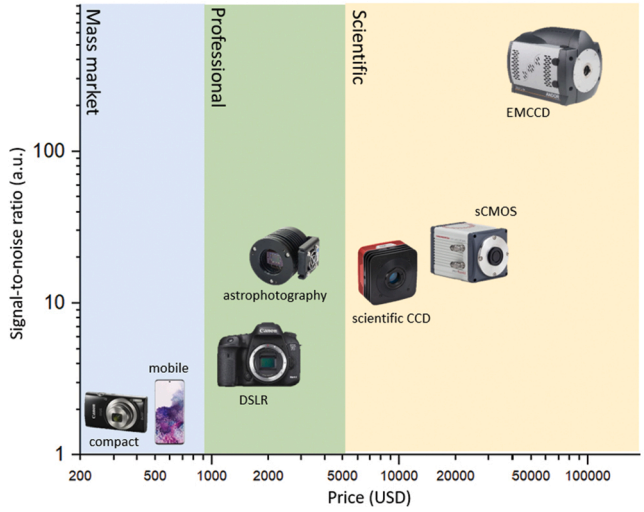

Fig. 1. Modern cameras overview: Signal-to-noise ratio estimated for 100 s exposition with 1 photon/pix/s light flux.

cost and small overall dimensions, (2) video cameras and cameras for amateur and professional movie filming and photography, incl. astrophotography, which allows obtaining high-quality images of objects, (3) cameras for scientific research, optimized for the reliable registration of small light fluxes, at a level of 10 photons and below during the exposure of one frame. One more important parameter of a CCD is the read-out noise, which, can be reduced by the specific statistical analysis of the data [22]. Modern CCD-cameras (especially with an internal electronic multiplication) allows highly sensitive [23] and rather fast [24] optical measurements. Far-field photoluminescence microscopy with a digital CCD-based signal detection starts to be very useful instrument in various research fields and scientific applications [25].

For the detection of weak light fluxes in a wide field luminescent microscopy setup, high-cost scientific cameras are used. They are based on charge coupled device (CCD) or complementary metal–oxidesemiconductor (CMOS) sensors [26,27]. Modern design of such detectors imply high quantum efficiency of photosensitive elements, low readout noise, low thermal noise, as well as built-in amplification systems for optical signals such as electronic multiplication of the recorded signal (EMCCD) [28,29,30].

To date, the progress in microelectronics has made it possible to significantly reduce the cost of the main element of cameras - a 2D photo-recording sensor [31,32,33]. From the comparison shown in Fig. 1, it can be seen that professional CCD cameras allow reaching the signal to noise ratio (SNR) as high, as certain scientific grade CCD cameras, but having a significantly lower price. With the price of 5000 USD, these cameras are based on highly efficient sensors, having quantum efficiency (QE) up to 70% and low noise levels. The possibility of using cheaper CCD cameras is extremely important in optical microscopy and spectroscopy research. It allows: (1) reducing the cost of an experimental setup, (2) increasing the availability of related experimental research, (3) reducing the cost of potential technological devices associated with the use of single photon sources (SPS) [34]. The use of low-cost cameras (both CCD and CMOS) is a trend of modern photonics [35].

In this work we study the possibility of using such cameras for highly sensitive measurements. We measure the weak optical response from single quantum emitters with a CCD camera for amateur astrophotography (Starlight Express Trius SX674), which has a high quantum efficiency and low thermal and readout noises. For comparison, the measurements were taken simultaneously with Andor iXon scientific EMCCD camera. Areas of applicability of the CCD camera for amateur astrophotography in optical microscopy of SPS are discussed.

2. Comparison of amateur astrophotography and scientific grade emCCD cameras

The signal detection in a CCD camera is based on the light-induced generation of electron-hole (e-h) pairs in the light-sensitive semiconductor elements (pixels) of the CCD camera sensor and subsequent accumulation of charges in those pixels. An image retrieved from the camera is a result of a charge readout from each pixel of the camera. The quality of an image is determined by the presence of noise that occurs at different stages of image acquisition. There are three main sources of noise: (1) camera readout noise, (2) shot noise of fluctuations in the number of photons hitting the camera, (3) thermal noise of the photosensitive elements of the camera sensor [36]. The typical values of the *readout noise* for modern scientific and professional CCD cameras are in the range of 3–40 photoelectrons per readout. It is mainly determined by the readout frequency, the electrical components of the amplifiers, as well as the implemented circuitry architecture. Typically, the readout noise is weakly dependent on external factors, thus its reduction is barely impossible. *Shot noise* depends on the number of registered photons N as $\sqrt{N}$ and does not depend on characteristics of the camera. The contribution of shot noise to the measured signal becomes equal to 10% when the number of photons is equal to 100, which imposes a fundamental restriction on the detection of weak optical signals with a total number of photocounts less than this value. *Thermal (or dark) noise* is associated with the charge generation due to thermal fluctuations in a semiconductor. This noise is determined by the material, structure and geometric dimensions of the camera sensor.

Surface defects in semiconductors, especially at the Si-SiO_2 interface, lead to the appearance of dark noise due to the creation of additional surface levels in the semiconductor band gap. Such surface noise is the dominant source of the dark signal. This noise can be eliminated using various surface preparation techniques. Similarly, defects in the bulk of a semiconductor create additional levels in the semiconductor band gap and contribute to the formation of e-h pairs inside the photosensitive element [37]. The overall rate of generation and recombination of e-h pairs formed through such additional levels can be represented by the expression:

$$U = \frac{\sigma_p \sigma_n \nu_{th} \left(pn - n_i^2\right) N_t}{\sigma_n \left[n + n_i \exp\left(\frac{E_t - E_i}{kT}\right)\right] + \sigma_p \left[p + n_i \exp\left(\frac{E_i - E_t}{kT}\right)\right]}, \quad (1)$$

where $\sigma_p, \sigma_n$are the holes and electrons capture cross sections, ν_{th} – the thermal velocity, p, n – the holes and electrons concentrations, N_t – the concentration of defects on the energy level E_t, E_i, n_i is the Fermi energy and concentration of the charge carriers in semiconductor. At the thermal equilibrium in a semiconductor the following condition is valid: $pn - n_i^2 = 0$, which means the equality in the number of generated and recombined pairs.

When light hits the CCD camera sensor, electrons accumulate in the potential well of the corresponding sensitive element of the CCD, and holes transit to the p-type region of the semiconductor. In this process, a charge depleted region is formed, i.e. $pn - n_i^2 \ll 0$. The electron-hole generation rate in the pixel with the area A_{pix} and linear dimension of depleted region x_{dep} can be written as

$$De_{dep}^{-} = \frac{x_{dep} A_{pix} n_i}{2\tau(T)} \quad (2)$$

where $\tau(T)$ is the time of electron-hole generation and T is the temperature of the pixel.

Besides, there are CCD sensor areas that are not exposed to light, but act as sources of a diffusion current, which leads to additional accumulation of electrons in pixel potential wells. The diffusion rate can be represented as

$$De^{-}_{diff} = \frac{D_n A_{pix} n_i^2}{x_c N_a} \quad (3)$$

where x_c is the size of the non-sensitive region of the pixel and D_n is the electron diffusion constant.

Thermal noise of the photosensitive element is proportional to the exposure time and its area and introduces a significant limitation for the measurements with long exposure times. Thermal noise is a combination of the above components, which depends on the temperature of the photosensitive element, and can be greatly reduced by cooling the camera CCD sensor. Best attainable values of such type of noise ranges from 0.001 photoelectrons to 1 photoelectron per second per pixel.

In the present work, we used an affordable CCD camera for amateur astrophotography Starlight Express Trius SX674 (hereinafter SX CCD), which uses the Sony ICX674 CCD sensor created using Super HAD CCD II technology. This technology made it possible to significantly reduce the thermal noise of the CCD sensor photosensitive elements, and reduce the manufacturing cost [38] which resulted in a wide variety of applications [39]. The SX CCD sensor uses an additional layer of p-type semiconductor with a high content of impurities (Hole Accumulation Diode, HAD), which significantly reduces thermal noise associated with the presence of semiconductors surface defects. However, the small pixel size of the CCD sensor severely restricts the light flux reaching each pixel due to the low numerical aperture determined by the pixel size. For this reason, the microlens array surfaced on a CCD sensor was introduced in order to increase the pixels numerical aperture. The array is located in such a way that each CCD pixel is in the focal plane of the corresponding microlens. This made it possible to double the collection angle per pixel of the CCD camera [40] and, thus, significantly increase the photon flux per pixel [41]. Using this approach, it is possible to achieve high QE of photosensitive elements (up to 77%) and at the same time low values of the dark current up to 0.004 photoelectrons per second per pixel when the CCD sensor is cooled to moderate temperatures, about −25 °C. These characteristics make SX CCD camera attractive for weak optical signals detection.

Table 1 shows a comparison of the technical characteristics of the SX CCD camera and the significantly more expensive Andor iXon Ultra (DU-897U-CS0-BVF) scientific camera with an electron signal multiplication (hereinafter scientific CCD, EM CCD), which has proven itself in optical measurements of single quantum light sources [42,29,43].

The EM CCD camera has the photoelectron multiplication function (there is no such function in the SX CCD), which means that the signal from each pixel of the CCD sensor is amplified prior to the signal readout process. This makes it possible to reduce the value of the root-mean-square (RMS) deviation of the effective readout noise to values significantly less than 1 and, as a consequence, to increase the signal-to-noise ratio (SNR) at short exposure times. At the same photon fluxes and longer exposure times, the use of EM does not lead to an increase in SNR. This is due to the fact that the signal amplification is a random process and, thus, introduces an additional error to the measured signal. This additional noise, associated with the signal amplification process, is increased with the number of registered photons N as $\sqrt{N}$. At long exposures, such noise is comparable or even exceeds the readout noise. It should be noted that the use of avalanche amplification of photoelectrons leads to a proportional decrease in the dynamic range of the CCD camera, since it is determined by the depths of the potential wells of the CCD photosensitive elements, as well as the readout and gain elements (the deeper the well, the greater the dynamic range), the analog-to-digital converter bit depth (the higher the bit depth, the greater the dynamic range) and the used signal amplification (when using amplification, the dynamic range is proportionally reduced). Thus, the EM mode is primarily used for low signal detection (from a few to several tens of photons per pixel), e.g. the measurements of the dynamics of a luminescence signal from single emitters with the exposure time less than 1 s.

In this work, both cameras were used for measurements with exposures longer than 1 s, for which there is no need to use the EM mode of the EM CCD **scientific** camera, which leads to an additional noise (to reduce read noise, the ADC speed was reduced to 80 kHz). As seen from Table 1, SX CCD has one order of magnitude smaller depth of pixels potential well as well as 12 times smaller pixel area. However, using 3 × 3 pixels binning, these parameters for the resulting “macro-pixel” will correspond to the characteristics of the Andor iXon camera. To compensate the existing difference in the pixels’ sizes of the cameras we used different optical magnification for each camera to get identical image sizes on both cameras. Since the pixel binning was carried out on the CCD sensor before the signal readout process, this does not lead to a significant increase in the signal readout noise from the macropixel. However, during pixel binning, the dark current of each pixel is summed leading to a greater dark current of macropixel compared to a single pixel. This results in a nine-fold increase in the dark current (up to 0.036 e- / pix / s) and, accordingly, a three-fold increase in the RMS of dark noise. Fig. 2 shows the measured dependence of RMS of the CCDs noises as a function of exposure time. In the figure we also show how the measured RMS signal depends on the effective area of CCD cameras used. In the post measured analysis, we excluded from the recorded CCD images signals corresponded to the so called “bad” pixels (hot or cold pixels). This procedure leads to the reduction of the effective CCD sensor area, as is denoted on the Fig. 2 as CCD working area. As shown in the figure, the measured RMS signals of both cameras are several times

Table 1
Comparison of main technical characteristics of SX CCD and emCCD cameras.

Characteristic	CCD for astrophotography (SX CCD)	Scientific CCD (EM mode off, 80 kHz)
Quantum efficiency @600 nm, %	70%	95%
Potential well depth, e^-	17,000	183,000
AD gain, e^-/CCD count	0.3	1.41
Pixel size, μm × μm	4.54×4.54	16×16
Macropixel size (3 × 3 binning), μm × μm	13.62×13.62	–
Readout noise, RMS, e^-	5.7	2.95
CCD sensor temperature, typ, °C	−25	−60
Dark current, e^-/pix/s	0.004 (0.036 – for macropixel)	0.01
Price, USD	3,000	70,000

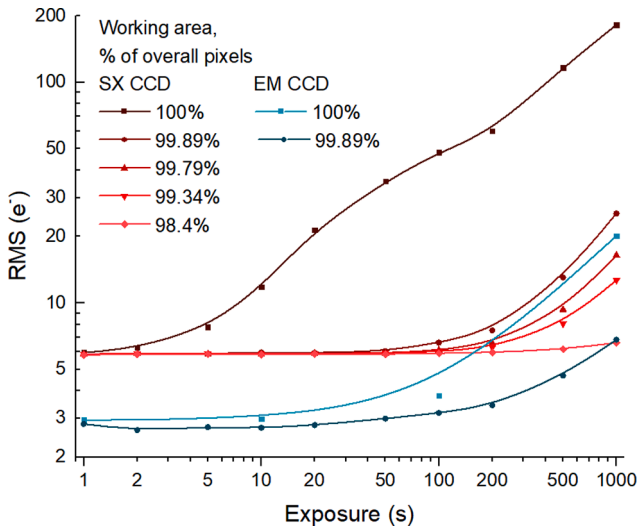

Fig. 2. CCD dark noise on background images captured with different exposure times: SX CCD (reds) and EM CCD (blues). Working area represents the percentage of source image pixels remaining after the correction of “bad” pixels (hot or cold pixels).

different (higher for the SX CCD) at low exposure times, while become practically the same at expositions longer than 500 s. Also note much higher impact of "bad" pixels into RMS signal of images recorded with the SX CCD.

In our measurements, we used the factory settings for the CCD sensor cooling systems: for the SX CCD camera the CCD sensor temperature was maintained at −25 °C, and for the scientific CCD the CCD sensor temperature was −60 °C. Both cameras were identically isolated from external light. Exposure times ranged from 1 s to 1000 s.

3. Materials and methods

Colloidal CdSeS/ZnS quantum dots (Sigma Aldrich, 753793), diameter d = 6 nm, spectral position of the luminescent peak – 630 nm, FWHM ~ 15 nm, luminescence lifetime ~ 20 ns were used as quantum light emitters. A sample with quantum dots (QDs) on a cover glass was prepared using the spincoating technique from a highly diluted colloidal solution of QDs in toluene.

The experimental setup used for the measurements is shown in Fig. 3 and has been described in details in [29]. The sample was fixed on a microscope stage with a three-dimensional piezo translation module (Nano Scan Technology). The second harmonic generation from a femtosecond pulsed laser (Avesta TEMA) was used to excite QDs photoluminescence (PL). The excitation laser wavelength was 525 nm, the pulse duration was extended to 1.8 ps, and the repetition rate was 72 MHz. The average intensity of the incident radiation on the sample varied from 20 mW/cm^2 to 67 W/cm^2 and was lower than the saturation intensity of the QDs optical transition.

QD PL was collected with Carl Zeiss 100x oil immersion objective (NA = 1.3) For the given NA and the optical magnification of the objective, the diffraction-limited spot (~250 nm) could be either imaged onto ~ 12 pixels/macropixels of CCD cameras or detected by 2 single photon avalanche photodiodes (SPADs). QD PL was filtered from the scattered laser light using a bandpass filter (Semrock 628/32). The collected QD PL was split in a 50:50 ratio using a beam splitter (Thorlabs BSW10). Achromatic doublets (Thorlabs AC254-125/150-A) were used to focus the radiation on the sensors of CCD cameras. Taking into account the quantum efficiency of detectors, The collection efficiency of photons from QDs, was ~ 15% for the scientific camera, and ~ 10.5% for SX CCD, and ~ 9.5% for SPADs. This estimate includes a geometrical factor - the fraction of radiation entering the microscope objective; anisotropy of radiation, including an increase in the fraction of radiation in a plane with a high refractive index; losses on optical elements of setup; quantum efficiency of detectors.

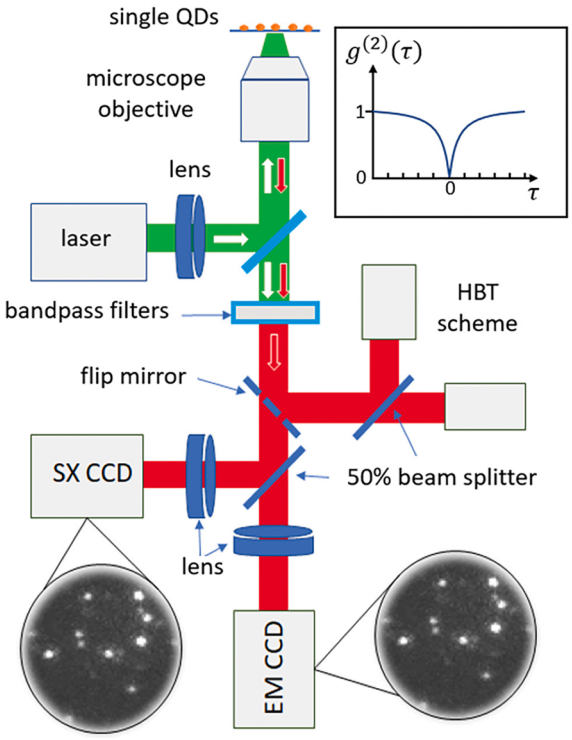

Fig. 3. A scheme of the experimental setup: the CCD-based single-molecule fluorescence nanoscope.

Due to the diffraction limitation, the optical images obtained by each of the cameras do not allow to distinguish a single QD from QDs agglomerates since in both cases, the optical image is limited by the Abbe diffraction limit. The simplest and most reliable way to distinguish a single quantum emitter from agglomerates is to measure the second-order correlation function $g^{(2)}(\tau)$ [44,45]. If the value of $g^{(2)}(0) \ll 1$, then the radiation source is a single quantum emitter, since in this case the probability of detecting two photons emitted simultaneously from a single quantum emitter is extremely low.

To measure the $g^2(\tau)$ function, we used Hanbury-Brown and Twiss (HBT) scheme [46] implemented in the optical scheme of the microscope (Fig. 3). Avalanche photodiodes EG&G SPCM 200 with a quantum efficiency of 60% at a wavelength of 630 nm, dark noise ~ 20 Hz, and a control board (Becker & Hickl 16-channel TCSPC module (DPC 230) with a temporal resolution of 165 ps) were used as fast detectors.

Fig. 4a and b show PL images of a sample with QDs obtained with both CCD cameras under the same excitation conditions (excitation intensity 67 W/cm^2, which is 50× lower than the saturation intensity of the optical transition for these QDs) [47]. The images were obtained with a relatively short exposure time of CCD cameras, equal to 1 s. The images were recorded with a short time delay (<1 s) on both CCD cameras which causes a small difference in PL images in Fig. 4 a, b

As can be seen from Fig. 4, both cameras display an identical area of the sample with QDs. Obtained image consists of light spots corresponding to light emitting objects with sizes smaller than the diffraction limit (~λ/2NA). Using the HBT scheme, we found QDs whose radiation corresponded to the radiation of SPS. One of those dots is highlighted in the Fig. 4 a and b with a red circle, and the cross section of the optical image of this spot is shown in Fig. 4c, d. The measured correlation function $g^{(2)}(\tau)$ of the light source corresponding to this QD is shown in Fig. 4e. A clearly dip at a zero-time delay $\tau = 0$, with the corresponding value $g^{(2)}(\tau) = 0.1$, indicates that this emitter is a single quantum emitter. Thus, the measurement results represented in Fig. 4, convincingly show the possibility of detecting the single quantum emitter luminescence with the astrophotography SX CCD camera.

We carried out a detailed analysis of the images obtained from the sample using both cameras. The main studied parameter was the ratio of the measured optical signal to the noise associated with the operation of the camera (readout noise and dark noise). Therefore, we did not take into account the shot noise of the signal itself, which in our experiments exceeded the total camera noise by more than an order of magnitude. To measure SNR, a single QD was selected in the image, that was captured by both cameras. Optical signal from a single QD was integrated over 12 pixels/macropixels of the QD image. The number of pixels and their relative position were optimized in terms of increasing the SNR [48], anomalous "hot" and "cold" pixels were eliminated. The dependency of overall noise before and after bad pixels corrections is represented in Fig. 2. From the obtained value, a constant signal (bias) set by the camera manufacturer was subtracted. Thus, for determining the signal-to-noise ratio of the image, the following expression was used:

$$SNR = \frac{Signal}{Noise} = \frac{(CCDcounts - N_{pix} \times bias)}{S_{Noise}} \quad (4)$$

where N_{pix} is a number of image pixels/macropixels. The noise S_{Noise} was found as RMS deviation of the signal integrated over 12 pixels outside the laser pump spot.

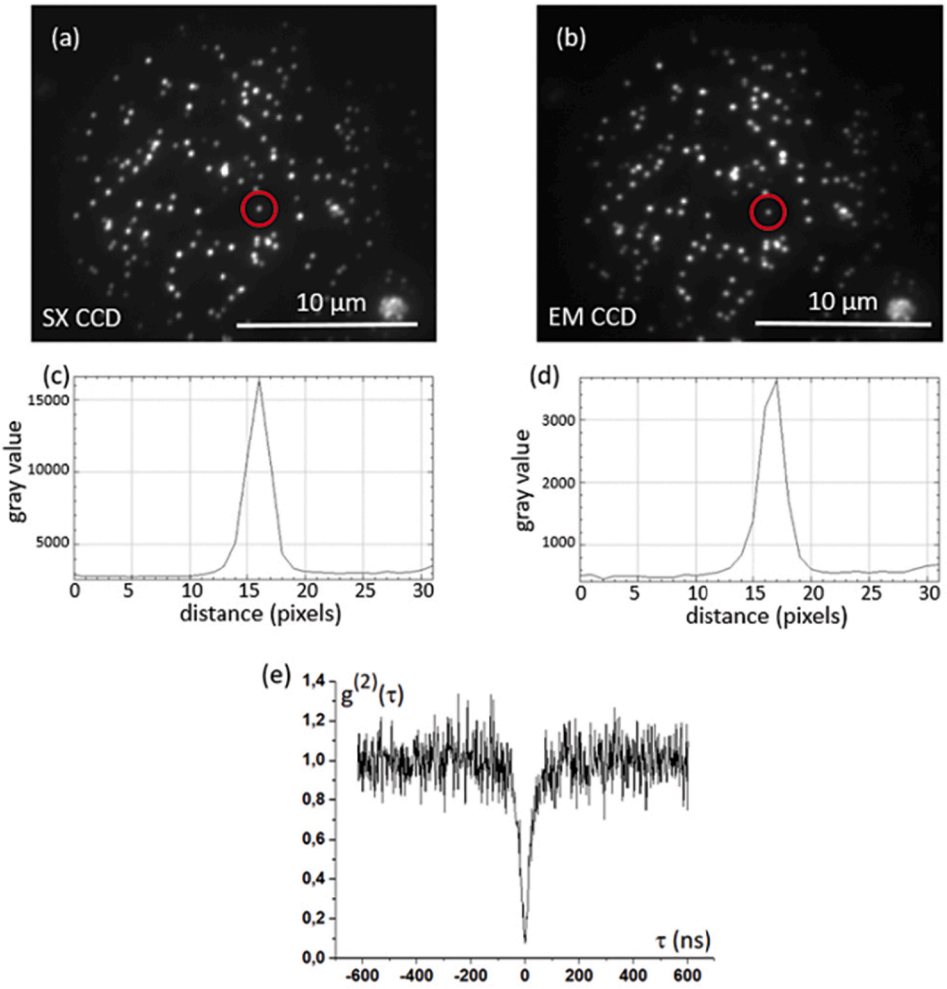

Fig. 4. Fluorescence images of the sample with single colloidal quantum dots CdSeS/ZnS at 1 s exposition: (a) astrophotography CCD (SXCCD) and (b) scientific grade CCD (EMCCD). (c),(d) cross sections of images of the same single QD obtained by both cameras – images (a) and (b) correspondingly, the QD is indicated by red circles on both images. (e) $g^2(\tau)$ correlation function of the indicated QD.

4. Results and discussion

Table. 2 shows the results of a comparison of the measured SNRs of a single QD images obtained with both cameras. It can be seen that at low exposure times the main noise source is the readout noise of the CCD matrix.

Results show that using both CCD cameras with an exposure time of 1 s allows to obtain an image of a single QD. In this case, both cameras recorded a flux from a single QD, approximately equal to 6×10^4 photons / s, which corresponds to the expected estimates of signal, considering the collection efficiency of a microscope and the quantum yield of QD luminescence.

To compare images from both cameras at significantly longer time exposures, we used an optical signal source with a photon flux about 4000 times less than the photon flux from a single QD in the previous experiment. To do this, we strongly decreased the average intensity of the exciting laser to a value of about 20 mW/cm^2. This value is almost five orders of magnitude less than the saturation intensity of the optical transition of the QDs, which leads to a proportional decrease in the photon flux from a single QD.

At the selected excitation intensities, images of single QDs were obtained at 1000 s exposure times with an acceptable SNR level (Fig. 5). Note that even at such large exposures, dark noise has not yet made a dominant contribution to the total noise. It increased for SX CCD macropixel from 5.7 photoelectrons to 12 photoelectrons for images with 1 s and 1000 s exposures, respectively. This increase in the noise is due to the appearance of dark current noise and hot pixels at long exposures. In this experiment, the SNR for the scientific CCD camera was 365, while for the SX CCD camera it was 161. The obtained absolute SNR values show the possibility of recording very low light fluxes with a long exposure. The minimum recorded photon flux using the SX CCD was about 10 photons/s (distributed over 12 macropixels), and was obtained in measurements with exposure times of 1000 s. Note that the registration of such a small photon flux is already sufficient for measuring the fluorescence spectrum of single quantum emitters. Thus, at long exposure times, a significant advantage of SX CCD cameras is the low level of dark noise which allows them to outperforms existing sCMOS cameras, and is comparable to scientific CCD cameras.

Table 2
SNR measurements for SX CCD and scientific grade CCD.

Camera, exposure time	CCD counts (a. u.)	Bias (a. u.)	Signal (e^-)	Noise (e^-)	SNR
CCD for astrophotography (SX CCD), 1 s	84,207	22,030	18,653	19.73	945
Scientific grade CCD, 1 s	25,713	2409	32,858	10.46	3141
CCD for astrophotography (SX CCD), 1000 s	44,920	21,864	6916	42.87	161
Scientific grade CCD (EM CCD), 1000 s	9122	2640	9334	25.59	365

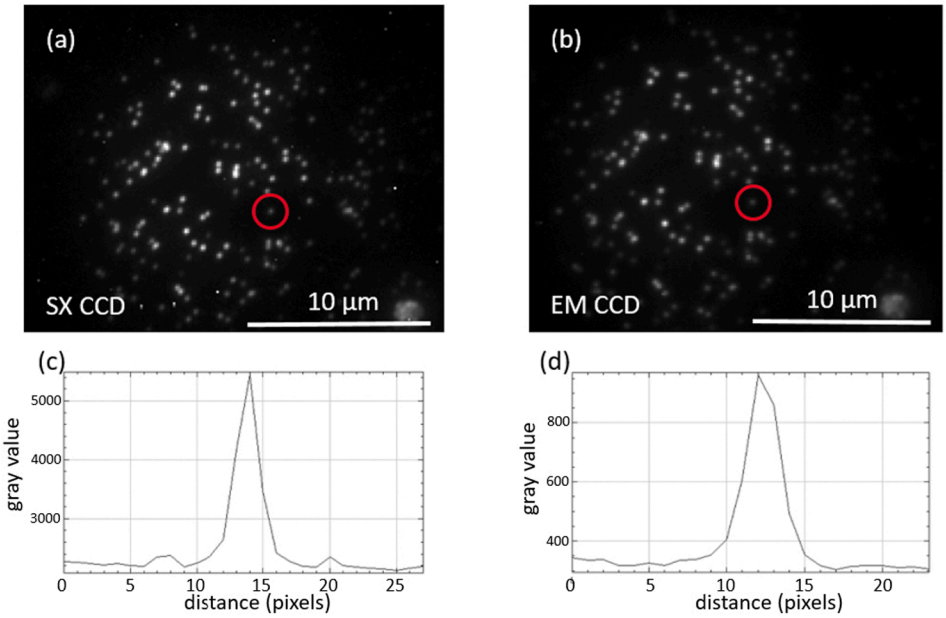

Fig. 5. (a)-(b) Optical image of the sample with single colloidal quantum dots CdSeS/ZnS at 1000 s exposition: (a) astrophotography CCD (SXCCD) and (b) scientific grade CCD (EMCCD). (c),(d) cross sections of images of the same single QD obtained by both cameras – images (a) and (b) correspondingly, the QD is indicated by red circles on both images.

5. Conclusions

The current level of technology allows creating CCD cameras with a relatively low cost and efficient enough to carry out optical microscopy and spectroscopy measurements with single quantum emitters of light.

Scientific EM CCDs are indispensable for studying the dynamics of quantum emitters especially in the conditions when the recorded signal becomes less than the readout noise. The electronic multiplication of the signal increases the SNR by reducing the contribution of readout noise to the overall signal. Comparative tests of cameras for amateur astrophotography SX CCD and scientific EM CCD were performed. EM CCD can reliably register low light fluxes of individual quantum emitters at rather small exposures, significantly less than 1 s, which turns out to be impossible using cheaper SX CCD. However, at large exposures, more than 1 s, CCDs for astrophotography allows achieving comparable values of the SNR to the scientific EM CCDs due to the technological solutions used, which can significantly reduce the dark noise of the astrophysical CCDs together with high quantum efficiency. The minimum flux of photons recorded by the astrophysical camera was 10 photons/s. Thus, it has been shown that modern amateur grade CCD cameras allow observing objects with small signals, such as single semiconductor quantum dots, organic dye molecules, color centers in diamond, emitting micro- and nanoparticles, etc. Moreover, such cameras are more affordable than specialized scientific cameras, opening up the opportunity to study quantum objects for a much wider range of research laboratories as well as in bio-sensing, based on the use of single-molecules-counting technique [49].

6. Contributions

A.G. and I.E. performed the experiment on the setup made by I.E. and A.N., A.G. performed data analysis and prepared the manuscript. A.N. developed software for image processing. P.M. conceived the original idea of the experiment and made important corrections of the manuscript. V.B. and A.N. supervised the project. All authors discussed the results and commented on the manuscript.

Declaration of Competing Interest

The authors declare that they have no known competing financial interests or personal relationships that could have appeared to influence the work reported in this paper.

Acknowledgements

A.G. and P.M acknowledge Russian Foundation for Basic Research (20-32-90070, 20-02-00059), V.B. acknowledges Russian Foundation for Basic Research (19-02-00207) for the support of experimental studies of spectromicroscopy of semiconductor colloidal quantum dots and their small ensembles. AN and IE acknowledge also Russian Foundation for Basic Research for support of studies in the field of fluorescence nanoscopy of macromolecules (20-03-00923).

Th[]among the State Contract of the Moscow Pedagogical State University (MPGU) “Physics of the perspective materials and nanostructures: basic researches and applications in material sciences, nanotechnologies and photonics” supported by the Ministry of Education of the Russian Federation (AAAA-A20-120061890084-9) in collaboration with the Centre of collective usage “Structural diagnostics of materials” of the Federal Research Center RAS “Crystallography and photonics”.

References

[1] V. Ahtee, R. Lettow, R. Pfab, A. Renn, E. Ikonen, S. Gotzinger, V. Sandoghdar, Molecules as sources for indistinguishable single photons, J. Mod. Opt. 56 (2009) 161–166.
[2] Y.M. Sigal, R.B. Zhou, X.W. Zhuang, Visualizing and discovering cellular structures with super-resolution microscopy, Science 361 (2018) 880–887.
[3] A. von Diezmann, Y. Shechtman, W.E. Moerner, Three-dimensional localization of single molecules for super resolution imaging and single-particle tracking, Chem. Rev. 117 (2017) 7244–7275.
[4] J.J. Gooding, K. Gaus, Single-molecule sensors: challenges and opportunities for quantitative analysis, Angew. Chem.-Int. Edit. 55 (2016) 11354–11366.
[5] A.V. Naumov, A.A. Gorshelev, Y.G. Vainer, L. Kador, J. Kohler, Far-field nanodiagnostics of solids with visible light by spectrally selective imaging, Angew. Chem.-Int. Edit. 48 (2009) 9747–9750.
[6] A.V. Naumov, Low-temperature spectroscopy of organic molecules in solid matrices: from the Shpol’skii effect to laser luminescent spectromicroscopy for all effectively emitting single molecules, Phys. Usp. 56 (2013) 605–622.

[7] A. Naumov, I.Y. Eremchev, A.A. Gorshelev, Laser selective spectromicroscopy of myriad single molecules: tool for far-field multicolour materials nanodiagnostics, Eur. Phys. J. D 68 (2014).
[8] Y.G. Vainer, A.V. Naumov, M. Bauer, L. Kador, Isotope effect in the linewidth distribution of single-molecule spectra in doped toluene at 2 K, J. Lumin. 127 (2007) 213–217.
[9] H. Xu, C.M. Liu, Y. He, H.W. Tang, Q.S. Wu, Study on the chemiluminescence resonance energy transfer between luminol and fluorescent dyes using a linear CCD spectrometer, J. Lumin. 130 (2010) 1872–1879.
[10] F. Jelezko, J. Wrachtrup, Single defect centres in diamond: A review, Phys. Status Solidi A-Appl. Mat. 203 (2006) 3207–3225.
[11] P.N. Melentiev, A.E. Afanasiev, A.A. Kuzin, V.M. Gusev, O.N. Kompanets, R. O. Esenaliev, V.I. Balykin, Split hole resonator: A nanoscale UV light source, Nano Lett. 16 (2016) 1138–1142.
[12] A. Merdasa, Y. Tian, R. Camacho, A. Dobrovolsky, E. Debroye, E.L. Unger, J. Hofkens, V. Sundstrom, I.G. Scheblykin, "Supertrap" at Work: Extremely Efficient Nonradiative Recombination Channels in MAPbI(3) Perovskites Revealed by Luminescence Super-Resolution Imaging and Spectroscopy, ACS Nano 11 (2017) 5391–5404.
[13] M. Nirmal, B.O. Dabbousi, M.G. Bawendi, J.J. Macklin, J.K. Trautman, T.D. Harris, L.E. Brus, Fluorescence intermittency in single cadmium selenide nanocrystals, Nature 383 (1996) 802–804.
[14] I.S. Osad'ko, Blinking fluorescence of single semiconductor nanocrystals: basic experimental facts and theoretical models of blinking, Phys. Usp. 59 (2016) 462–474.
[15] A.E. Krasnok, I.S. Maksymov, A.I. Denisyuk, P.A. Belov, A.E. Miroshnichenko, C. R. Simovski, Y.S. Kivshar, Optical nanoantennas, Phys. Usp. 56 (2013) 539–564.
[16] V.I. Balykin, P.N. Melentiev, Optics and spectroscopy of a single plasmonic nanostructure, Phys. Usp. 61 (2018) 133–156.
[17] S. Cazaux, A. Sadoun, M. Biarnes-Pelicot, M. Martinez, S. Obeid, P. Bongrand, L. Limozin, P.H. Puech, Synchronizing atomic force microscopy force mode and fluorescence microscopy in real time for immune cell stimulation and activation studies, Ultramicroscopy 160 (2016) 168–181.
[18] B.C. Fitzmorris, J.K. Cooper, J. Edberg, S. Gul, J.H. Guo, J.Z. Zhang, Synthesis and structural, optical, and dynamic properties of core/shell/shell CdSe/ZnSe/ZnS quantum dots, J. Phys. Chem. C 116 (2012) 25065–25073.
[19] S.J. LeBlanc, M.R. McClanahan, M. Jones, P.J. Moyer, Enhancement of multiphoton emission from single CdSe quantum dots coupled to gold films, Nano Lett. 13 (2013) 1662–1669.
[20] T. Plakhotnik, W.E. Moerner, V. Palm, U.P. Wild, Single-molecule spectroscopy - maximum emission rate and saturation intensity, Opt. Commun. 114 (1995) 83–88.
[21] L. Sapienza, M. Davanco, A. Badolato, K. Srinivasan, Nanoscale optical positioning of single quantum dots for bright and pure single-photon emission, Nat Commun 6 (2015).
[22] J.C. Mullikin, L.J. Vanvliet, H. Netten, F.R. Boddeke, G. Vanderfeltz, I.T. Young, Methods for Ccd Camera Characterization, Image Acquisition Scientific Imaging Syst. 2173 (1994) 73–84.
[23] K. Sperlich, H. Stolz, Quantum efficiency measurements of (EM)CCD cameras: high spectral resolution and temperature dependence, Meas. Sci. Technol. 25 (2014).
[24] R. Geisler, A fast multiple shutter for luminescence lifetime imaging, Meas. Sci. Technol. 28 (2017).
[25] K. Karimullin, M. Knyazev, I. Eremchev, Y. Vainer, A. Naumov, A tool for alignment of multiple laser beams in pump-probe experiments, Meas. Sci. Technol. 24 (2013).
[26] M. Haruta, Y. Fujiyoshi, T. Nemoto, A. Ishizuka, K. Ishizuka, H. Kurata, Extremely low count detection for EELS spectrum imaging by reducing CCD read-out noise, Ultramicroscopy 207 (2019).
[27] F. Huang, T.M.P. Hartwich, F.E. Rivera-Molina, Y. Lin, W.C. Duim, J.J. Long, P. D. Uchil, J.R. Myers, M.A. Baird, W. Mothes, M.W. Davidson, D. Toomre, J. Bewersdorf, Video-rate nanoscopy using sCMOS camera-specific single-molecule localization algorithms, Nat. Methods 10 (2013) 653-+.
[28] M. Barbiero, S. Castelletto, X.S. Gan, M. Gu, Spin-manipulated nanoscopy for single nitrogen-vacancy center localizations in nanodiamonds, Light-Sci. Appl. 6 (2017).
[29] I.Y. Eremchev, M.Y. Eremchev, A.V. Naumov, Multifunctional far-field luminescence nanoscope for studying single molecules and quantum dots (50th anniversary of the Institute of Spectroscopy, Russian Academy of Sciences), Phys. Usp. 62 (2019) 294–303.
[30] C.J. Picken, R. Legaie, J.D. Pritchard, Single atom imaging with an sCMOS camera, Appl. Phys. Lett. 111 (2017).
[31] E.R. Fossum, D.B. Hondongwa, A Review of the Pinned Photodiode for CCD and CMOS Image Sensors, IEEE J. Electron Devices Soc. 2 (2014) 33–43.
[32] N. Stuurman, R.D. Vale, Impact of new camera technologies on discoveries in cell biology, Biol. Bull. 231 (2016) 5–13.
[33] R. Walczak, W. Kubicki, J. Dziuban, Low cost fluorescence detection using a CCD array and image processing for on-chip gel electrophoresis, Sens. Actuator B-Chem. 240 (2017) 46–54.
[34] I. Gerhardt, L.J. Mai, A. Lamas-Linares, C. Kurtsiefer, Detection of single molecules illuminated by a light-emitting diode, Sensors 11 (2011) 905–916.
[35] D.J. Duke, T. Knast, B. Thethy, L. Gisler, D. Edgington-Mitchell, A low-cost high-speed CMOS camera for scientific imaging, Meas. Sci. Technol. 30 (2019).
[36] G.E. Healey, R. Kondepudy, Radiometric Ccd camera calibration and noise estimation, IEEE Trans. Pattern Anal. Mach. Intell. 16 (1994) 267–276.
[37] R. Widenhorn, M.M. Blouke, A. Weber, A. Rest, E. Bodegom, Temperature dependence of dark current in a CCD, Sens. Camera Syst. Scientific, Ind., Digital Photogr. Appl. Iii 4669 (2002) 193–201.
[38] Y. Kitano, H. Abe, J. Kuroiwa, K. Hirata, H. Ohki, N. Karasawa, R. Takizawa, M. Yamashita, M. Sato, K. Kokubun, Method of driving solid state image sensing device, in: G. Patent (Ed.), 2009.
[39] A.J.P. Theuwissen, The hole role in solid-state imagers, IEEE Trans. Electron Devices 53 (2006) 2972–2980.
[40] H.L. Martin, Method for directly scanning a rectilinear imaging element using a non-linear scan, in: G. Patent (Ed.), 2001.
[41] Y. Okazaki, Y. Tomiya, Microlens array and method of forming same and solid-state image pickup device and method of manufacturing same., in: G. Patent (Ed.), 2000.
[42] A.S. Backer, M.P. Backlund, M.D. Lew, W.E. Moerner, Single-molecule orientation measurements with a quadrated pupil, Opt. Lett. 38 (2013) 1521–1523.
[43] S. Khan, N.C. Verma, A. Gupta, C.K. Nandi, Reversible photoswitching of carbon dots, Sci. Rep. 5 (2015).
[44] R. Loudon, The Quantum Theory of Light, 3rd ed., Oxford University Press, Oxford; New York, 2000.
[45] C.T. Yuan, P. Yu, H.C. Ko, J. Huang, J. Tang, Antibunching single-photon emission and blinking suppression of CdSe/ZnS quantum dots, ACS Nano 3 (2009) 3051–3056.
[46] J.I. Gonzalez, T.H. Lee, M.D. Barnes, Y. Antoku, R.M. Dickson, Quantum mechanical single-gold-nanocluster electroluminescent light source at room temperature (vol 93, art no 147402, 2004), Phys. Rev. Lett. 93 (2004).
[47] I.Y. Eremchev, I.S. Osad'ko, A.V. Naumov, Auger ionization and tunneling neutralization of single CdSe/ZnS nanocrystals revealed by excitation intensity variation, J. Phys. Chem. C 120 (2016) 22004–22011.
[48] I.Y. Eremchev, N.A. Lozing, M.G. Gladush, A.A. Bayev, A.A. Rozhentsov, A. V. Naumov, Measuring fluctuations in the intensity of a single point-like luminescence emitter: artifacts in processing microscopic images, Bull. Russ. Acad. Sci. Phys. 82 (2018) 1482–1486, https://doi.org/10.3103/S1062873818080166.
[49] P.N. Melentiev, L.V. Son, D.S. Kudryavtsev, I.E. Kasheverov, V.I. Tsetlin, R.O. Esenaliev, V.I. Balykin, Ultrafast, ultrasensitive detection and imaging of single cardiac troponin-T molecules, ACS Sens. 5 (2020) 3576–3583.